Original Article | Thoracic Imaging

eISSN 2005-8330
https://doi.org/10.3348/kjr.2020.0592
Korean J Radiol 2021;22(3):464-475

Korean Journal of Radiology
KJR

Volume and Mass Doubling Time of Lung Adenocarcinoma according to WHO Histologic Classification

Jung Hee Hong, MD[1], Samina Park, MD[2], Hyungjin Kim, MD, PhD[1], Jin Mo Goo, MD, PhD[1, 3], In Kyu Park, MD, PhD[2], Chang Hyun Kang, MD, PhD[2], Young Tae Kim, MD, PhD[2], Soon Ho Yoon, MD, PhD[1]

Departments of [1]Radiology and [2]Thoracic and Cardiovascular Surgery, Seoul National University College of Medicine, Seoul National University Hospital, Seoul, Korea; [3]Institute of Radiation Medicine, Seoul National University Medical Research Center, Seoul, Korea

Objective: This study aimed to evaluate the tumor doubling time of invasive lung adenocarcinoma according to the International Association of the Study for Lung Cancer (IASLC)/American Thoracic Society (ATS)/European Respiratory Society (ERS) histologic classification.

Materials and Methods: Among the 2905 patients with surgically resected lung adenocarcinoma, we retrospectively included 172 patients (mean age, 65.6 ± 9.0 years) who had paired thin-section non-contrast chest computed tomography (CT) scans at least 84 days apart with the same CT parameters, along with 10 patients with squamous cell carcinoma (mean age, 70.9 ± 7.4 years) for comparison. Three-dimensional semiautomatic segmentation of nodules was performed to calculate the volume doubling time (VDT), mass doubling time (MDT), and specific growth rate (SGR) of volume and mass. Multivariate linear regression, one-way analysis of variance, and receiver operating characteristic curve analyses were performed.

Results: The median VDT and MDT of lung cancers were as follows: acinar, 603.2 and 639.5 days; lepidic, 1140.6 and 970.1 days; solid/micropapillary, 232.7 and 221.8 days; papillary, 599.0 and 624.3 days; invasive mucinous, 440.7 and 438.2 days; and squamous cell carcinoma, 149.1 and 146.1 days, respectively. The adjusted SGR of volume and mass of the solid-/micropapillary-predominant subtypes were significantly shorter than those of the acinar-, lepidic-, and papillary-predominant subtypes. The histologic subtype was independently associated with tumor doubling time. A VDT of 465.2 days and an MDT of 437.5 days yielded areas under the curve of 0.791 and 0.795, respectively, for distinguishing solid-/micropapillary-predominant subtypes from other subtypes of lung adenocarcinoma.

Conclusion: The tumor doubling time of invasive lung adenocarcinoma differed according to the IASCL/ATS/ERS histologic classification.

Keywords: *Adenocarcinoma of lung; Lung cancer; Tomography; Diagnostic imaging*

INTRODUCTION

Lung cancer is the leading cause of cancer-related death worldwide, accounting for one out of five (18.4%) of all such deaths (1). A major histologic classification of lung cancer comprises adenocarcinoma, squamous cell carcinoma, small cell carcinoma, and large cell carcinoma. Lung adenocarcinoma is the most common histologic type of lung cancer, of which the relative proportion has gradually increased since the 1970s (2). Additionally, lung adenocarcinoma is a primary histologic type that is treatable using molecular targeted therapies against driver mutations (3). Furthermore, the early detection of lung adenocarcinoma—relative to other histologic types—has been the main contributor to the survival benefit of low-dose computed tomography (CT) screening for lung cancer (4).

The growth rate of lung cancer is an important prognostic biomarker reflecting the malignant potential of the tumor (5, 6). Although lung adenocarcinoma typically grows more slowly than lung squamous cell carcinoma or small

Received: February 17, 2020 **Revised:** June 11, 2020
Accepted: June 13, 2020
Corresponding author: Soon Ho Yoon, MD, PhD, Department of Radiology, Seoul National University College of Medicine, Seoul National University Hospital, 101 Daehak-ro, Jongno-gu, Seoul 03080, Korea.
• E-mail: yshoka@gmail.com

Korean Journal of Radiology
KJR

cell carcinoma, the growth rate of adenocarcinoma ranges widely, with a tumor doubling time from a few months to years (7-11). The presence of ground-glass opacities, which are common in lepidic-predominant adenocarcinoma and rare in solid- or micropapillary-predominant subtypes, are known to partly contribute to the variation in the growth rate of adenocarcinoma (9, 12).

Lung adenocarcinoma comprises several histologic subtypes, which may also result in the variation in the growth rate of adenocarcinoma. Primary invasive lung adenocarcinoma is currently categorized into six subtypes according to its predominant histologic features based on the 2011 classification of the International Association of the Study for Lung Cancer (IASLC)/American Thoracic Society (ATS)/European Respiratory Society (ERS): lepidic-predominant, acinar-predominant, papillary-predominant, solid-predominant, and micropapillary-predominant adenocarcinoma as well as variants of invasive adenocarcinoma including invasive mucinous, colloid, enteric, and fetal adenocarcinomas (13). This categorization reflects a prognostic divergence in lung adenocarcinoma, as solid or micropapillary-predominant adenocarcinoma shows worse clinical outcomes, with a higher incidence of locoregional recurrence and lymph node metastasis, than other subtypes of lung adenocarcinoma, whereas lepidic-predominant adenocarcinoma has more favorable outcomes (14-17).

This study aimed to evaluate the volume doubling time (VDT) and mass doubling time (MDT) of invasive lung adenocarcinoma according to the 2011 IASCL/ATS/ERS histologic classification.

MATERIALS AND METHODS

This retrospective study was approved by our Institutional Review Board, and informed consent was waived (IRB No. H1807-108-959).

Study Population

From January 2013 to June 2019, 2905 consecutive adult patients underwent curative surgical resection for primary lung adenocarcinoma at a single tertiary hospital. Among these patients, we applied the following inclusion criteria to determine eligibility: patients with 1) primary invasive lung adenocarcinoma, 2) patients with non-contrast chest CT scans with a slice thickness of less than 1.25 mm and no overlapping sections, and 3) patients with available pair of non-contrast chest CT scans obtained at least 84 days (12 weeks) apart with the same CT parameters, including the reconstruction algorithm, kernel, and slice thickness (18). We excluded patients with 1) endobronchial lung cancer, 2) no identifiable tumor on the interval CT scan, and 3) a history of chemotherapy or chemoradiation therapy before surgery. We also excluded patients with atypical adenomatous hyperplasia, adenocarcinoma *in situ*, minimally invasive adenocarcinoma, or mixed invasive mucinous and non-mucinous adenocarcinoma (Fig. 1).

Consequently, a total of 172 patients (mean age, 65.6 ± 9.0 years; 105 males and 67 females) were included in this study. The distribution of lung adenocarcinoma subtypes was as follows: lepidic-predominant, 26; acinar-predominant, 77; papillary-predominant, 41; solid-predominant, 16; micropapillary-predominant, 1; and invasive mucinous adenocarcinoma (IMA), 11. For comparison, we additionally included lung cancer patients with squamous cell carcinoma (n = 10; mean age, 70.9 ± 7.4 years; 10 males) with the same inclusion and exclusion criteria.

CT Acquisition

All chest CT scans were performed using one of the seven multi-detector CT scanners with 16 or more channels (Sensation 16, SOMATOM Definition, Siemens Heathineers, Brilliance-64, Ingenuity, Philips Healthcare, Aquilion One, Toshiba Medical Systems, Discovery CT750HD, LightSpeed Ultra, GE Healthcare). The CT protocol, reconstruction algorithm, kernel, slice thickness, and presence of slice overlap or inter-slice gap were identical for each pair of CT scans of all included patients. Consequently, the paired CT scans of most patients were obtained using the same CT apparatus, except for 13 patients in which the scans were performed using different CT scanners. The median time interval between the pairs of CT scans was 472.5 days (interquartile range [IQR], 238.0–833.3) without statistically significant difference between adenocarcinoma subtypes (acinar predominant, median 434.0 days [IQR, 260.0–833.0]; lepidic predominant, median 496.5 days [IQR, 218.0–1099.0]; solid predominant, median 623.0 days [IQR, 367.0–979.0]; papillary predominant, median 545.0 days [IQR, 272.0–797.0]; IMA, median 580.0 days [IQR, 378.5–1360.0]; $p = 0.875$). Most of the CT examinations were performed with a fixed tube voltage of 120 kVp with automatic exposure control, and the CT images were obtained in a craniocaudal direction during a single full-inspiratory breath-hold.

 https://doi.org/10.3348/kjr.2020.0592

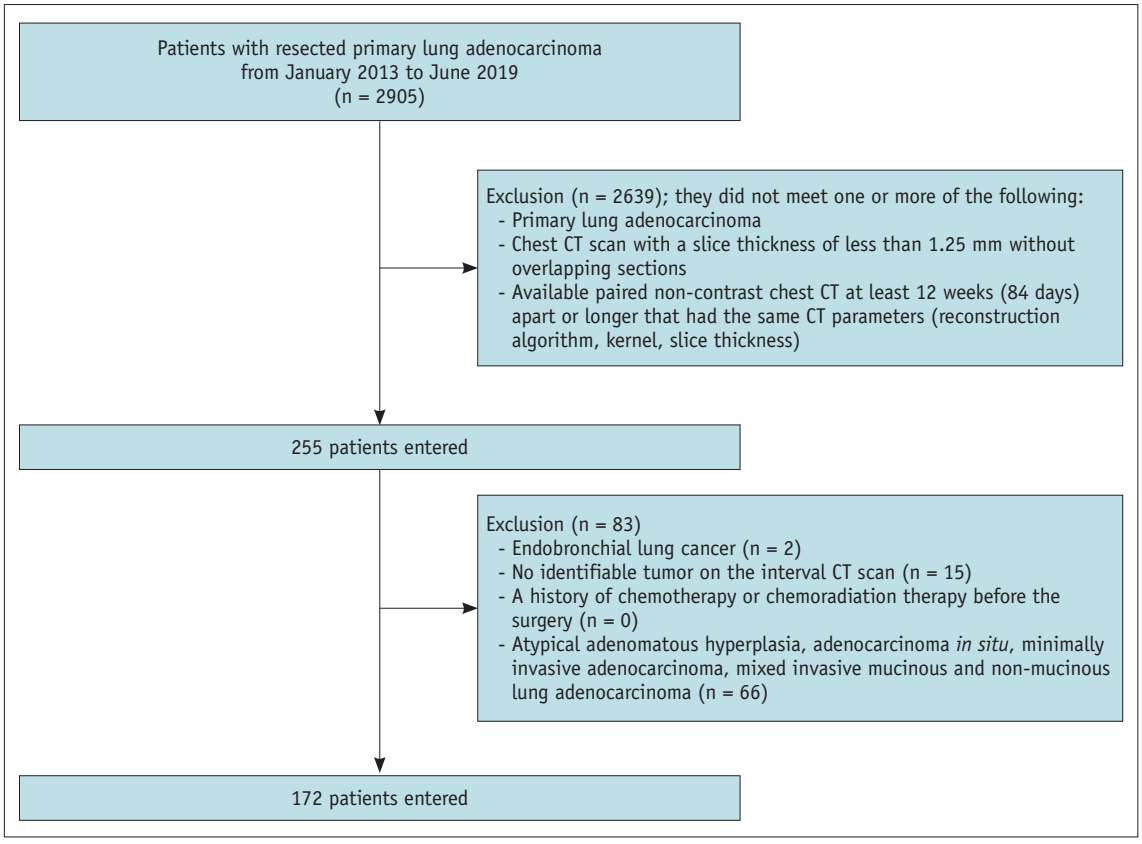

Fig. 1. Patient inclusion flowchart. CT = computed tomography

CT Analysis

One chest radiologist (with 6 years of experience in thoracic CT) performed three-dimensional semiautomatic segmentation of the tumors using commercially available software (IntelliSpace Portal version 10.1.1, Philips Healthcare). In each pair of CT scans, the earlier CT scan was considered to be the baseline CT scan, whereas the later one was analyzed as the follow-up CT scan. After uploading the Digital Imaging and Communication in Medicine data of the thin-section chest CT images, the software automatically detected and segmented the lung nodules three-dimensionally. The radiologist visually inspected the result of the segmentation in axial, coronal, and sagittal reconstruction images and determined the appropriateness of the segmentation. The results of the automatic segmentation were appropriate and accepted without adjustment in most cases, whereas manual adjustment was applied minimally by the radiologist in a limited number of patients (23 patients, 13.4%). After completing the segmentation, the software automatically calculated the volume and mass of the segmented nodule, along with determining the mean CT attenuation.

The VDT and MDT of the growing nodule were calculated using a method based on the modified Schwartz formula of an exponential growth model as follows: VDT or MDT = (log2 x T)/(log [X_s/X_f]), where T is the time interval between a pair of CT scans and X_s and X_f are the second and first volumes or masses of a lung nodule from a pair of CT scans, respectively (19). There were 10 cases of negative VDTs in our study, which was not rare in several previous studies due to some degree of uncertainty depending on factors related to measurement (7, 8, 20-25). Therefore, in univariate and multivariate linear regression analyses performed to investigate the factors associated with the doubling time of lung adenocarcinoma, we used specific growth rate (SGR) instead of VDT or MDT, which is already proven as more accurate and intuitive to represent tumor growth including negative values, and the equation of the SGR is as follows: SGR = log2/VDT or log2/MDT (26).

The radiologist evaluated the radiologic characteristics of the nodule on the follow-up CT scan. The nodule density was classified into three categories: pure ground-glass nodules, part-solid nodules, and solid nodules. In terms of CT morphology, the presence of air bronchogram, bubble

https://doi.org/10.3348/kjr.2020.0592

Korean Journal of Radiology
KJR

lucency, cavitation, notch, lobulated border, spiculation, and roundness were evaluated (27-29).

Histologic Evaluation

According to the IASLC/ATS/ERS classification, the ratio of the histological pattern of surgically resected lung adenocarcinoma was recorded in 5% increments in the pathology report (13). The predominant subtype that occupied most of the tumor was determined to be lepidic, acinar, papillary, solid, or micropapillary. Lung adenocarcinoma can be graded using a modified system according to the predominant histologic subtype as follows (30, 31): acinar-predominant invasive adenocarcinoma (group I), lepidic-predominant invasive adenocarcinoma (group II), solid-/micropapillary-predominant invasive adenocarcinoma (group III), papillary-predominant invasive adenocarcinoma (group IV), and IMA (group V). Cases with solid or micropapillary components that occupied no less than 5% but were not predominant were defined as minor components. Lymphovascular invasion was reported when tumor cells were demonstrated by the presence of tumor cells in lymphatic channels, veins, and arteries.

Statistical Analyses

We used the chi-squared test to compare categorical variables and the Pearson correlation coefficient and the Kruskal-Wallis test to compare continuous variables. The Dunn test with the Bonferroni correction was applied as a post hoc analysis. We used univariate linear regression analysis to investigate factors associated with the tumor growth rate of lung adenocarcinoma. Multivariate linear regression was applied to identify the independent variables associated with the tumor growth rate. Variables with a significance level of $p < 0.25$ in the univariate analysis were selected for inclusion in the multivariate linear regression models. To identify whether the existence of solid/micropapillary subtypes as a minor component affected tumor growth, intergroup comparisons between the three groups divided according to the percentage of solid/micropapillary subtypes used a one-way ANOVA with Tukey post hoc analysis. We constructed a receiver operating characteristic (ROC) curve and calculated the area under the curve (AUC) to identify the optimal cutoff values of VDT and MDT for the differentiation of the solid/micropapillary predominant subtype from other subtypes of lung adenocarcinoma (model 1) and for the differentiation of the solid/micropapillary predominant subtypes and squamous cell carcinoma from other subtypes of lung adenocarcinoma (model 2).

A p value less than 0.05 was considered statistically significant. All analyses were performed using the SPSS version 23 (International Business Machines Corp.) and R statistical software (R version 3.5.1., http://www.R-project.org/).

RESULTS

Baseline Characteristics

The median volume change of 172 included invasive adenocarcinomas was 80.3% (range, -98.3% to 27000.9%). The 10 squamous cell carcinomas showed an overall median volume change of 69.4% (range, -6.4% to 1258.9%). Smoking status, sex, CT characteristics of the nodule, bubble lucency, cavity, and the presence of a spiculated border were significantly different across the histologic subtypes of lung adenocarcinoma (Table 1). The solid/micropapillary subtypes were common in current or former smokers (15 of 17, 88.2%), men (16 of 17, 94.1%), and solid-type nodules (13 of 17, 76.5%), whereas bubble lucency and spiculated borders were common in acinar-predominant adenocarcinomas (15 of 77, 19.5% and 28 of 77, 36.4%, respectively). Air bronchogram, pure ground-glass nodules, and part-solid nodules were frequent in the lepidic-predominant subtype (18 of 26, 69.2%; 6 of 26, 23.1%; and 19 of 26, 73.1%, respectively).

VDT and MDT of Invasive Lung Adenocarcinoma

For nodules approximately 5 mm or smaller ([longest diameter: median, 4.9 mm; IQR, 3.1–5.2 mm], [volume, median, 23.2 mm^3; IQR, 12.9–44.5 mm^3]), the mass and density of nodules could not be computed using the software, since these measures were not sufficiently reliable in such small nodules. Accordingly, the MDT could be calculated for a total of 163 nodules (154 adenocarcinoma nodules and 9 squamous cell carcinoma nodules) (Table 2).

The VDT and MDT were significantly different across the lung adenocarcinoma subtypes ($p < 0.001$). The median VDT of the solid/micropapillary predominant subtype (232.7 days) was significantly shorter than those of the acinar-, lepidic-, and papillary-predominant subtypes (median VDT, 603.2, 1140.6, and 599.0 days, respectively), except IMA subtype (median VDT, 440.7 days). Similar results were obtained for the MDT: the solid-/micropapillary-predominant subtypes (median MDT, 221.8 days) showed

 https://doi.org/10.3348/kjr.2020.0592

significantly faster growth than the acinar-, lepidic-, and papillary-predominant subtypes, except for the IMA subtype (median MDT of the acinar-predominant, lepidic-predominant, papillary-predominant, and IMA subtypes, 639.5, 970.1, 624.3, and 438.2 days, respectively) (Tables 2, 3, Figs. 2, 3).

When adding the squamous cell carcinomas in addition to lung adenocarcinoma, the squamous cell carcinomas (median VDT and MDT, 149.1 and 146.1 days, respectively) showed significantly faster growth in both VDT and MDT than the acinar-, lepidic-, and papillary-predominant subtypes of adenocarcinoma. However, the squamous cell carcinomas showed faster growth in MDT only than the IMA (Tables 2, 3). There was no significant difference in both VDT and MDT between the squamous cell carcinoma and solid-/micropapillary-predominant subtypes. However, the solid-/micropapillary-predominant subtypes of adenocarcinoma showed significantly faster growth in both VDT and MDT

Table 1. Clinical and Radiological Characteristics of 172 Patients with Lung Adenocarcinoma

	All Patients	Acinar Predominant	Lepidic Predominant	Solid/ Micropapillary Predominant	Papillary Predominant	IMA	*P*
Number	172	77	26	17	41	11	
Age*	65.6 ± 9.0	64.8 ± 9.0	63.0 ± 9.5	69.1 ± 7.8	66.6 ± 8.7	67.5 ± 8.8	0.099
Smoking†	88 (51.2)	38 (49.4)	9 (34.6)	15 (88.2)	21 (51.2)	5 (45.5)	0.014
Pack-year‡	20.0 (0.0–35.0)	20.0 (0.0–35.0)	2.0 (0.0–17.5)	40.0 (20.0–40.0)	20.0 (6.0–30.0)	20.0 (4.0–35.0)	
Sex†							0.045
Male	105 (61.0)	45 (58.4)	14 (53.8)	16 (94.1)	25 (61.0)	5 (45.5)	
Female	67 (39.0)	32 (41.6)	12 (46.2)	1 (5.9)	16 (39.0)	6 (54.5)	
CT characteristics							0.001
Solid	62 (36.0)	26 (33.8)	1 (3.8)	13 (76.5)	17 (41.5)	5 (45.5)	
pGGN	19 (11.0)	6 (7.8)	6 (23.1)	1 (5.9)	5 (12.2)	1 (9.1)	
Part solid nodule	91 (52.9)	45 (58.4)	19 (73.1)	3 (17.6)	19 (46.3)	5 (45.5)	
Air bronchogram†	95 (55.2)	44 (57.1)	18 (69.2)	5 (29.4)	20 (48.8)	8 (72.7)	0.066
Bubble lucency†	18 (10.5)	15 (19.5)	0 (0.0)	0 (0.0)	3 (7.3)	0 (0.0)	0.009
Cavity†	2 (1.2)	0 (0.0)	0 (0.0)	1 (5.9)	0 (0.0)	1 (9.1)	0.027
Notch†	38 (22.1)	20 (26.0)	9 (34.6)	1 (5.9)	6 (14.6)	2 (18.2)	0.133
Round†	18 (10.5)	9 (11.7)	0 (0.0)	1 (5.9)	7 (17.1)	1 (9.1)	0.242
Spiculation†	43 (25.0)	28 (36.4)	5 (19.2)	3 (17.6)	7 (17.1)	0 (0.0)	0.023
Cancer history†	45 (26.2)	19 (24.7)	6 (23.1)	5 (29.4)	10 (24.4)	5 (45.5)	0.646
Lung cancer history†	21 (12.3)	11 (14.5)	1 (3.8)	1 (5.9)	7 (17.1)	1 (9.1)	0.451
Lymphovascular invasion	28 (16.3)	17 (22.1)	4 (15.4)	1 (5.9)	5 (12.2)	1 (9.1)	0.382

*Data are mean ± standard deviation, †Data are number of patients, with percentages in parentheses, ‡Data are median values, with IQR in parentheses. CT = computed tomography, IMA = invasive mucinous adenocarcinoma, IQR = interquartile range, pGGN = pure ground-glass nodule

Table 2. VDT and MDT Measurements of 182 Lung Cancers

	Acinar Predominant	Lepidic Predominant	Solid/Micropapillary Predominant	Papillary Predominant	IMA	Squamous Cell Carcinoma
VDT (days)						
Number	77	26	17	41	11	10
	603.2	1140.6	232.7	599.0	440.7	149.1
	(317.5–1067.3)	(447.1–2077.4)	(162.3–422.3)	(332.4–975.4)	(300.1–690.5)	(112.2–414.3)
MDT (days)						
Available number	67	25	14	39	9	9
	639.5	970.1	221.8	624.3	438.2	146.1
	(407.4–1268.9)	(625.2–1643.5)	(162.9–361.6)	(391.7–959.8)	(216.2–586.6)	(111.4–424.2)

Data are median values, with IQR in parentheses. MDT = mass doubling time, VDT = volume doubling time

https://doi.org/10.3348/kjr.2020.0592

Korean Journal of Radiology
KJR

Table 3. Adjusted *P* Values Using the Dunn Test with the Bonferroni Correction (A) between Different Histologic Subtypes of Lung Adenocarcinoma and (B) between Lung Cancer Types, Considering Squamous Cell Carcinoma in Addition to Lung Adenocarcinoma

P		SGR Volume	SGR Mass
A: Lung adenocarcinoma	Total	< 0.001	< 0.001
	Solid/micropapillary vs. acinar	< 0.001	< 0.001
	Solid/micropapillary vs. lepidic	< 0.001	< 0.001
	Solid/micropapillary vs. papillary	< 0.001	< 0.001
	Solid/micropapillary vs. IMA	0.141	0.241
B: Squamous cell carcinoma and lung adenocarcinoma	Total	< 0.001	< 0.001
	Solid/micropapillary vs. acinar	< 0.001	< 0.001
	Solid/micropapillary vs. lepidic	< 0.001	< 0.001
	Solid/micropapillary vs. papillary	< 0.001	< 0.001
	Solid/micropapillary vs. IMA	0.260	0.477
	Acinar vs. squamous cell carcinoma	< 0.001	< 0.001
	Lepidic vs. squamous cell carcinoma	< 0.001	< 0.001
	Solid/micropapillary vs. squamous cell carcinoma	1.000	0.495
	Papillary vs. squamous cell carcinoma	0.004	< 0.001
	IMA vs. squamous cell carcinoma	0.271	0.019

acinar = acinar predominant adenocarcinoma, lepidic = lepidic predominant adenocarcinoma, papillary = papillary predominant adenocarcinoma, SGR = specific growth rate, solid/micropapillary = solid/micropapillary predominant adenocarcinoma, squamous cell carcinoma = squamous cell carcinoma of the lung

than the acinar-, lepidic-, and papillary-predominant subtype, except for the IMA subtype.

Clinicopathologic Predictors of Growth Rate in Lung Adenocarcinomas

For the analysis of SGR of volume, age, smoking history, sex, CT characteristics, air bronchogram, notch, lobulated border, and histologic subtype were adjusted in the multivariate linear regression model, with a significance level of $p < 0.25$. For the analysis of SGR of mass, age, smoking history, sex, CT characteristics, air bronchogram, bubble lucency, notch, cancer history, and histologic subtype were adjusted in the multivariate regression model (Supplementary Table 1). The multivariate analyses showed that the histologic subtype of lung adenocarcinoma showed significant correlations with both SGR of volume and mass (Tables 4, 5).

The group of solid/micropapillary subtype as a predominant component (n = 17) showed significantly shorter VDT and MDT than both groups of absence of solid/micropapillary component (n = 132) and presence of solid/micropapillary subtype as minor component (n = 23) (median VDT and MDT: solid/micropapillary subtype present as predominant component, 232.7 and 221.8 days; solid/micropapillary subtype present as minor component, 566.0 and 539.9 days; solid/micropapillary subtype absent, 630.5 and 678.3 days). In the one-way ANOVA with post hoc Tukey analysis, the group of solid/micropapillary subtype as a predominant component had more significantly different SGR volume and mass compared to the other two groups (Tables 6, 7).

The ROC curve analysis showed that solid-/micropapillary-predominant adenocarcinoma could be differentiated from the other subtypes of lung adenocarcinoma (model 1) with AUCs of 0.791 and 0.795 using VDT and MDT, respectively. Both solid-/micropapillary-predominant adenocarcinoma and squamous cell carcinoma were differentiated from the other subtypes of lung adenocarcinoma (model 2) with AUCs of 0.767 and 0.769 using VDT and MDT, respectively (Fig. 4).

In model 1, the optimal cutoff values of VDT and MDT were 465.2 days (sensitivity, 88.2%; specificity, 63.9%) and 437.5 days (sensitivity, 85.7%; specificity, 72.1%), respectively. In model 2, the optimal cutoff values of VDT and MDT were 254.1 days (sensitivity, 66.7%; specificity, 83.2%) and 437.5 days (sensitivity, 82.6%; specificity, 72.1%), respectively. In model 1, when we set the sensitivity at the 95th percentile level, the cutoff values of VDT and MDT were 514.7 days (specificity, 56.7%) and 901.1 days (specificity, 34.3%), respectively. When we set the specificity at the 95th percentile level, the cutoff values of VDT and MDT were 121.8 days (sensitivity, 23.5%) and 130.2 days (sensitivity, 21.4%), respectively.

 https://doi.org/10.3348/kjr.2020.0592

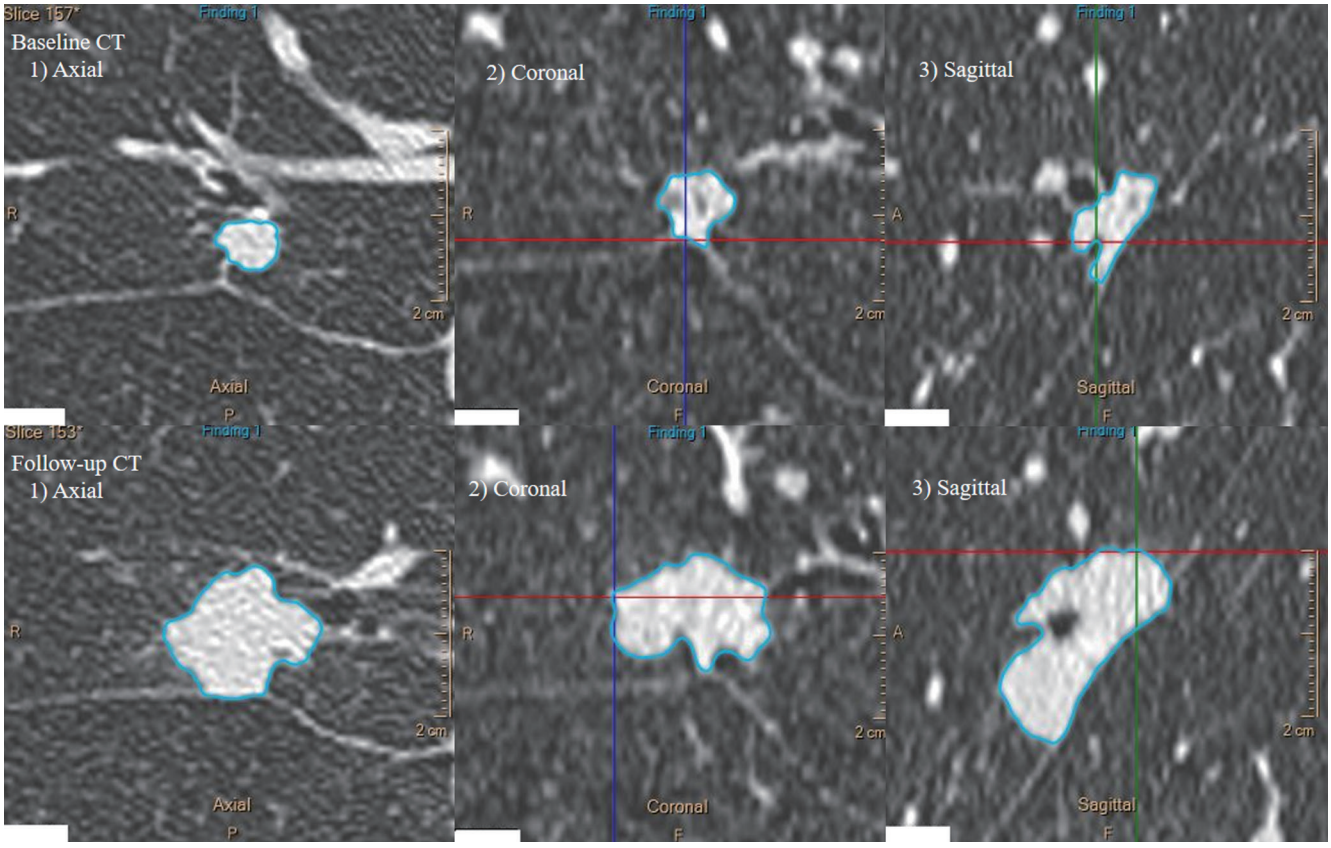

Fig. 2. A representative case of solid-predominant lung adenocarcinoma in the right middle lobe of an 80-year-old male patient.
During 469 days of follow-up, the nodule became enlarged, with a volume change of 292.5%. The calculated VDT and MDT were 232.7 and 224.7 days, respectively. MDT = mass doubling time, VDT = volume doubling time

DISCUSSION

The histologic classification of surgically resected lung adenocarcinoma is an independent prognostic factor (13, 15, 17). The pre-procedural identification of the IASLC/ATS/ERS histologic subtype may support appropriate, timely treatment strategies in the form of surgical resection, stereotactic radiation therapy, or tumor ablation (32-34). However, percutaneous core lung biopsy in predicting the histologic subtypes has limitation in an adequate separation of solid-/micropapillary-predominant subtypes from the other subtypes. The results of a biopsy may not represent the histologic pattern of the entire tumor (35). Additionally, biopsies may not be technically applicable to minute indeterminate pulmonary nodules smaller than 10 mm. In this context, a volumetric assessment of the tumor growth rate between interval CT scans may be of clinical value for guiding tailored treatment by identifying solid-/micropapillary-predominant histologic subtypes.

SGR of volume and mass of the solid-/micropapillary-predominant subtypes were shorter than those of other subtypes of adenocarcinoma and comparable to those of squamous cell carcinoma. The median VDT of the lepidic-predominant subtype was over 1000 days, which was significantly longer than that of other subtypes. Even after adjusting for the presence of ground-glass opacities, which have been suggested as contributing factor to tumor doubling time (8, 9), histologic subtype was a significant contributor to the tumor doubling time of lung adenocarcinoma. However, different from the predominant histologic components, the minor components of solid/micropapillary subtypes of lung adenocarcinoma did not have significant correlation with tumor doubling time. Considering that the minor components of solid/micropapillary subtypes were not influenced by the tumor doubling times, the major histologic subtype of lung adenocarcinoma seems to be a primary determinant of growth rate in lung adenocarcinoma, which can vary widely. Since tumor doubling time is considered as a prognostic factor reflecting tumor aggressiveness, the rapid growth of the solid-/micropapillary-predominant subtypes may partly explain their unfavorable prognosis.

https://doi.org/10.3348/kjr.2020.0592

Korean Journal of Radiology
KJR

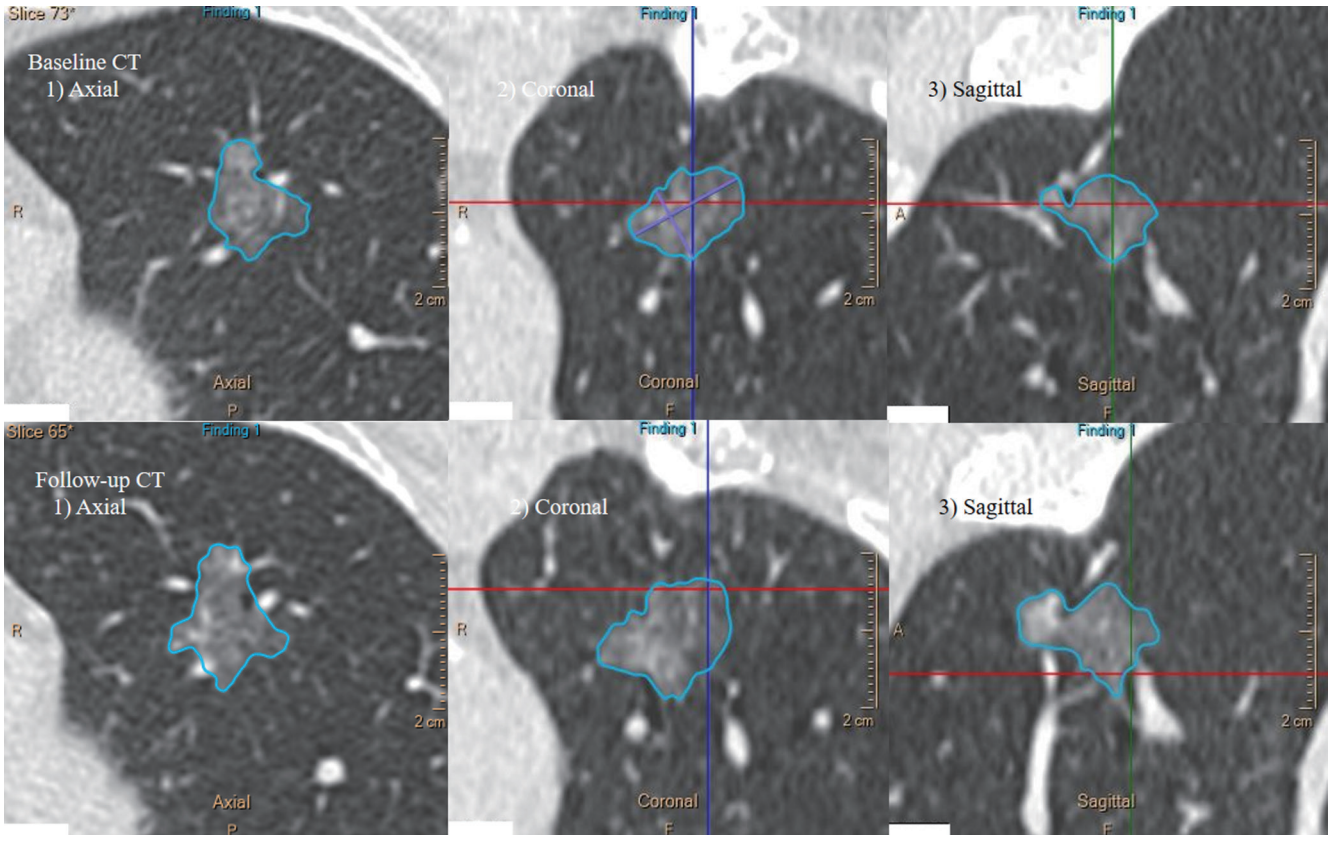

Fig. 3. A representative case of lepidic-predominant lung adenocarcinoma in the left upper lobe of a 66-year-old female patient. During 546 days of follow-up, the nodule became enlarged, with a volume change of 35.5%. The calculated VDT and MDT were 1244.4 and 1297.2 days, respectively.

Table 4. Univariate and Multivariate Linear Analyses for Prediction of SGR of Volume

	Univariate Anlysis				Multivariate Analysis*			
	B	95% CI		*P*	B	95% CI		*P*
WHO histologic classification								
Solid/micropapillary	Reference				Reference			
Acinar	-0.003162	-0.004330	-0.001993	< 0.001	-0.002652	-0.003882	-0.001423	< 0.001
Lepidic	-0.004721	-0.006081	-0.003362	< 0.001	-0.003889	-0.005377	-0.002402	< 0.001
Papillary	-0.002848	-0.004106	-0.001591	< 0.001	-0.002474	-0.003761	-0.001187	< 0.001
IMA	-0.001990	-0.003677	-0.000303	0.002	-0.001657	-0.003382	6.836710	0.060

*Adjusted by age, smoking history, sex, CT characteristics, air bronchogram, notch, and lobulated. CI = confidence interval

Table 5. Univariate and Multivariate Linear Analyses for Prediction of SGR of Mass

	Univariate Anlysis				Multivariate Analysis*			
	B	95% CI		*P*	B	95% CI		*P*
WHO histologic classification								
Solid/micropapillary	Reference				Reference			
Acinar	-0.003322	-0.004471	-0.002172	< 0.001	-0.002315	-0.003499	-0.001131	< 0.001
Lepidic	-0.003846	-0.005152	-0.002540	< 0.001	-0.002542	-0.003932	-0.001151	< 0.001
Papillary	-0.002902	-0.004121	-0.001683	< 0.001	-0.002108	-0.003311	-0.000905	< 0.001
IMA	-0.001733	-0.003405	-0.000062	0.042	-0.000914	-0.002547	0.000719	0.270

*Adjusted by age, smoking history, sex, CT characteristics, air bronchogram, bubble lucency, notch and cancer history.

https://doi.org/10.3348/kjr.2020.0592

Table 6. VDT and MDT according to Presence of Solid/Micropapillary Components

	Solid/Micropapillary Present as Predominant Component	Solid/Micropapillary Present as Minor Component	Solid/Micropapillary Subtype Absent	*P*
VDT (days)				< 0.001
Number	17	23	132	
	232.7 (162.3–422.3)	566.0 (356.2–870.7)	630.5 (349.9–1228.7)	
MDT (days)				0.001
Number	14	22	118	
	221.8 (162.9–361.6)	539.9 (401.0–779.2)	678.3 (419.6–1271.9)	

Data are median values, with IQR in parentheses.

Table 7. One-Way ANOVA with Post Hoc Tukey Test to Identify Minor Component of Solid/Micropapillary Subtypes Affect SGR of Volume and Mass

P	SGR Volume	SGR Mass
Intergroup comparison	< 0.001	< 0.001
S/M absent vs. S/M minor	0.999	0.938
S/M absent vs. S/M predominant	< 0.001	< 0.001
S/M minor vs. S/M predominant	< 0.001	< 0.001

S/M absent = solid/micropapillary subtype absent, S/M minor = solid/micropapillary subtype present as minor component, S/M predominant = solid/micropapillary subtype present as predominant component

One of the practical advantages of these results is that the cutoff values of VDT and/or MDT are potentially applicable to screening-detected early lung cancer with uniform interval CT scans. Interval follow-up CT scans are used to evaluate indeterminate pulmonary nodules in lung cancer screening programs such as the Dutch-Belgian Lung Cancer Screening (NELSON) trial or Lung-Reporting and Data System (Lung-RADS) (25, 36-38). The volume or mass change between interval CT scans is typically calculated to differentiate lung cancer from a benign pulmonary nodule (37, 38). The calculated volume or mass change of the nodule can also be compared with the appropriate cutoff value to differentiate solid-/micropapillary-predominant adenocarcinoma and squamous cell carcinoma from other subtypes of lung adenocarcinoma. Although small cell lung cancer was not included in this study, it grows rapidly, and the VDT and MDT of small cell lung cancer are usually more rapid than the cutoff values presented in this study (9). Thus, the volumetric assessment of nodule growth between interval CT scans may potentially determine the malignancy and certain subtypes of lung adenocarcinoma noninvasively.

Our study has several limitations. First, this study was conducted in a retrospective manner at a single institution. Second, the number of primary lung adenocarcinomas varied across histologic subtypes. In particular, there was only one case of the micropapillary-predominant subtype, which is a rare subtype. We classified solid- and micropapillary-predominant subtypes together (30), because both subtypes have high metastatic potential and poorer outcomes than other subtypes. Further studies to validate our results in a larger cohort are required. Third, the study only included surgically resected lung adenocarcinoma, potentially excluding extremely rapidly growing tumors for which surgical resection would be impossible. Fourth, interobserver measurement variability was not assessed. Nevertheless, double reading of the same chest CT scan rarely happens in clinical practice or low-dose chest CT screening. Our measurements tried to simulate those used in real practice settings, while minimizing potential sources of measurement variability, such as different CT parameters, different readers between scans, or manual measurements. The reader consistently used the same three-dimensional semiautomatic segmentation software without adjustment in most cases. Fifth, the software could not separate a subsegmental pulmonary vessel from a solid portion in calculating the volume and mass of subsolid nodules. Sixth, we have included all enrolled cases without specifying a volume change threshold in order not to exclude nodules with slow growth rates. Tumor volume measurements cannot avoid some degree of uncertainty associated with measurement techniques or readers (18, 20, 22). To reduce these errors, we matched the CT parameters, including the reconstruction algorithm, kernel, and slice thickness between baseline and follow-up CT scans and minimalized manual adjustment of segmentation. Consequently, the study population was inevitably reduced. A more extensive study containing CT scans with different CT parameters would be required to generalize our results.

In conclusion, the tumor doubling time of invasive lung adenocarcinoma differed according to the IASCL/ATS/ERS histologic subtype. The VDT and MDT, which are assessed between interval CT scans, may be used to noninvasively differentiate the solid-/micropapillary-predominant subtypes

https://doi.org/10.3348/kjr.2020.0592

Korean Journal of Radiology
KJR

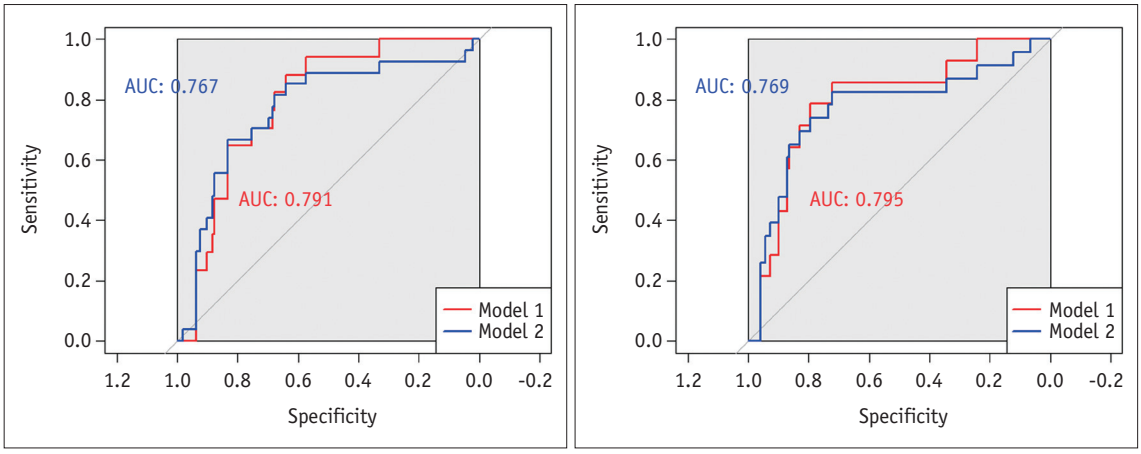

Fig. 4. The ROC curves of VDT and MDT for detecting solid- and micropapillary-predominant adenocarcinoma among lung adenocarcinoma subtypes (model 1) and for detecting both solid-/micropapillary-predominant adenocarcinoma and squamous cell carcinoma (model 2). The AUC of model 1, which solely included solid-/micropapillary-predominant subtypes, was greater than that of model 2, which included squamous cell carcinoma in addition to the solid-/micropapillary-predominant subtype (AUC of VDT, 0.791 vs. 0.767; AUC of MDT, 0.795 vs. 0.769, respectively).
A. The ROC curve of VDT for detecting solid-/micropapillary-predominant adenocarcinoma among lung adenocarcinoma subtypes (model 1) and for detecting both solid-/micropapillary-predominant adenocarcinoma and squamous cell carcinoma (model 2). **B.** The ROC curve of MDT for detecting solid-/micropapillary-predominant adenocarcinoma among lung adenocarcinoma subtypes (model 1) and for detecting both solid-/micropapillary-predominant adenocarcinoma and squamous cell carcinoma (model 2). AUC = area under the curve, ROC = receiver operating characteristic

of lung adenocarcinoma and squamous lung carcinoma from other subtypes of invasive lung adenocarcinomas, thereby guiding proper management strategies.

Supplementary Materials

The Data Supplement is available with this article at https://doi.org/10.3348/kjr.2020.0592.

Conflicts of Interest

The authors have no potential conflicts of interest to disclose.

ORCID iDs

Jung Hee Hong
https://orcid.org/0000-0002-4299-6411
Samina Park
https://orcid.org/0000-0001-9625-2672
Hyungjin Kim
https://orcid.org/0000-0003-0722-0033
Jin Mo Goo
https://orcid.org/0000-0003-1791-7942
In Kyu Park
https://orcid.org/0000-0003-3550-5554
Chang Hyun Kang
https://orcid.org/0000-0002-1612-1937
Young Tae Kim
https://orcid.org/0000-0001-9006-4881
Soon Ho Yoon
https://orcid.org/0000-0002-3700-0165

REFERENCES

1. Bray F, Ferlay J, Soerjomataram I, Siegel RL, Torre LA, Jemal A. Global cancer statistics 2018: GLOBOCAN estimates of incidence and mortality worldwide for 36 cancers in 185 countries. *CA Cancer J Clin* 2018;68:394-424
2. Meza R, Meernik C, Jeon J, Cote ML. Lung cancer incidence trends by gender, race and histology in the United States, 1973-2010. *PLoS One* 2015;10:e0121323
3. Chan BA, Hughes BG. Targeted therapy for non-small cell lung cancer: current standards and the promise of the future. *Transl Lung Cancer Res* 2015;4:36-54
4. Pinsky PF, Church TR, Izmirlian G, Kramer BS. The national lung screening trial: results stratified by demographics, smoking history, and lung cancer histology. *Cancer* 2013;119:3976-3983
5. Mizuno T, Masaoka A, Ichimura H, Shibata K, Tanaka H, Niwa H. Comparison of actual survivorship after treatment with survivorship predicted by actual tumor-volume doubling time from tumor diameter at first observation. *Cancer* 1984;53:2716-2720
6. Arai T, Kuroishi T, Saito Y, Kurita Y, Naruke T, Kaneko M. Tumor doubling time and prognosis in lung cancer patients: evaluation from chest films and clinical follow-up study. *Jpn J*

Clin Oncol 1994;24:199-204
7. Honda O, Johkoh T, Sekiguchi J, Tomiyama N, Mihara N, Sumikawa H, et al. Doubling time of lung cancer determined using three-dimensional volumetric software: comparison of squamous cell carcinoma and adenocarcinoma. *Lung Cancer* 2009;66:211-217
8. Mackintosh JA, Marshall HM, Yang IA, Bowman RV, Fong KM. A retrospective study of volume doubling time in surgically resected non-small cell lung cancer. *Respirology* 2014;19:755-762
9. Obayashi K, Shimizu K, Nakazawa S, Nagashima T, Yajima T, Kosaka T, et al. The impact of histology and ground-glass opacity component on volume doubling time in primary lung cancer. *J Thorac Dis* 2018;10:5428-5434
10. Wilson DO, Ryan A, Fuhrman C, Schuchert M, Shapiro S, Siegfried JM, et al. Doubling times and CT screen–detected lung cancers in the Pittsburgh Lung Screening Study. *Am J Respir Crit Care Med* 2012;185:85-89
11. Winer-Muram HT, Jennings SG, Tarver RD, Aisen AM, Tann M, Conces DJ, et al. Volumetric growth rate of stage I lung cancer prior to treatment: serial CT scanning. *Radiology* 2002;223:798-805
12. Lee HJ, Kim YT, Kang CH, Zhao B, Tan Y, Schwartz LH, et al. Epidermal growth factor receptor mutation in lung adenocarcinomas: relationship with CT characteristics and histologic subtypes. *Radiology* 2013;268:254-264
13. Travis WD, Brambilla E, Noguchi M, Nicholson AG, Geisinger KR, Yatabe Y, et al. International Association for the Study of Lung Cancer/American Thoracic Society/European Respiratory Society International Multidisciplinary Classification of Lung Adenocarcinoma. *J Thorac Oncol* 2011;6:244-285
14. Tsao MS, Marguet S, Le Teuff G, Lantuejoul S, Shepherd FA, Seymour L, et al. Subtype classification of lung adenocarcinoma predicts benefit from adjuvant chemotherapy in patients undergoing complete resection. *J Clin Oncol* 2015;33:3439-3446
15. Ujiie H, Kadota K, Chaft JE, Buitrago D, Sima CS, Lee MC, et al. Solid predominant histologic subtype in resected stage I lung adenocarcinoma is an independent predictor of early, extrathoracic, multisite recurrence and of poor postrecurrence survival. *J Clin Oncol* 2015;33:2877-2884
16. Wang L, Jiang W, Zhan C, Shi Y, Zhang Y, Lin Z, et al. Lymph node metastasis in clinical stage IA peripheral lung cancer. *Lung Cancer* 2015;90:41-46
17. Yoshizawa A, Sumiyoshi S, Sonobe M, Kobayashi M, Fujimoto M, Kawakami F, et al. Validation of the IASLC/ATS/ERS lung adenocarcinoma classification for prognosis and association with EGFR and KRAS gene mutations: analysis of 440 Japanese patients. *J Thorac Oncol* 2013;8:52-61
18. Devaraj A, van Ginneken B, Nair A, Baldwin D. Use of volumetry for lung nodule management: theory and practice. *Radiology* 2017;284:630-644
19. Schwartz M. A biomathematical approach to clinical tumor growth. *Cancer* 1961;14:1272-1294
20. Jennings SG, Winer-Muram HT, Tann M, Ying J, Dowdeswell I. Distribution of stage I lung cancer growth rates determined with serial volumetric CT measurements. *Radiology* 2006;241:554-563
21. Lindell RM, Hartman TE, Swensen SJ, Jett JR, Midthun DE, Tazelaar HD, et al. Five-year lung cancer screening experience: CT appearance, growth rate, location, and histologic features of 61 lung cancers. *Radiology* 2007;242:555-562
22. Quint LE, Cheng J, Schipper M, Chang AC, Kalemkerian G. Lung lesion doubling times: values and variability based on method of volume determination. *Clin Radiol* 2008;63:41-48
23. Field JK, Duffy SW, Baldwin DR, Whynes DK, Devaraj A, Brain KE, et al. UK Lung Cancer RCT Pilot Screening Trial: baseline findings from the screening arm provide evidence for the potential implementation of lung cancer screening. *Thorax* 2016;71:161-170
24. Pastorino U, Rossi M, Rosato V, Marchianò A, Sverzellati N, Morosi C, et al. Annual or biennial CT screening versus observation in heavy smokers: 5-year results of the MILD trial. *Eur J Cancer Prev* 2012;21:308-315
25. van Klaveren RJ, Oudkerk M, Prokop M, Scholten ET, Nackaerts K, Vernhout R, et al. Management of lung nodules detected by volume CT scanning. *N Engl J Med* 2009;361:2221-2229
26. Mehrara E, Forssell-Aronsson E, Ahlman H, Bernhardt P. Specific growth rate versus doubling time for quantitative characterization of tumor growth rate. *Cancer Res* 2007;67:3970-3975
27. Lee HJ, Goo JM, Lee CH, Park CM, Kim KG, Park EA, et al. Predictive CT findings of malignancy in ground-glass nodules on thin-section chest CT: the effects on radiologist performance. *Eur Radiol* 2009;19:552-560
28. Nakazono T, Sakao Y, Yamaguchi K, Imai S, Kumazoe H, Kudo S. Subtypes of peripheral adenocarcinoma of the lung: differentiation by thin-section CT. *Eur Radiol* 2005;15:1563-1568
29. Zwirewich CV, Vedal S, Miller RR, Müller NL. Solitary pulmonary nodule: high-resolution CT and radiologic-pathologic correlation. *Radiology* 1991;179:469-476
30. Sica G, Yoshizawa A, Sima CS, Azzoli CG, Downey RJ, Rusch VW, et al. A grading system of lung adenocarcinomas based on histologic pattern is predictive of disease recurrence in stage I tumors. *Am J Surg Pathol* 2010;34:1155-1162
31. Suh YJ, Lee HJ, Kim YT, Kang CH, Park IK, Jeon YK, et al. Added prognostic value of CT characteristics and IASLC/ATS/ERS histologic subtype in surgically resected lung adenocarcinomas. *Lung Cancer* 2018;120:130-136
32. Gao S, Stein S, Petre EN, Shady W, Durack JC, Ridge C, et al. Micropapillary and/or solid histologic subtype based on pre-treatment biopsy predicts local recurrence after thermal ablation of lung adenocarcinoma. *Cardiovasc Intervent Radiol* 2018;41:253-259
33. Leeman JE, Rimner A, Montecalvo J, Hsu M, Zhang Z, von Reibnitz D, et al. Histologic subtype in core lung biopsies of early-stage lung adenocarcinoma is a prognostic factor for

https://doi.org/10.3348/kjr.2020.0592

treatment response and failure patterns after stereotactic body radiation therapy. *Int J Radiat Oncol Biol Phys* 2017;97:138-145
34. Nitadori J, Bograd AJ, Kadota K, Sima CS, Rizk NP, Morales EA, et al. Impact of micropapillary histologic subtype in selecting limited resection vs lobectomy for lung adenocarcinoma of 2cm or smaller. *J Natl Cancer Inst* 2013;105:1212-1220
35. Huang KY, Ko PZ, Yao CW, Hsu CN, Fang HY, Tu CY, et al. Inaccuracy of lung adenocarcinoma subtyping using preoperative biopsy specimens. *J Thorac Cardiovasc Surg* 2017;154:332-339.e331
36. American College of Radiology. Lung CT screening reporting and data system (Lung-RADS). Acr.org Web site. https://www.acr.org/Clinical-Resources/Reporting-and-Data-Systems/Lung-Rads. Accessed January 8, 2020
37. Han D, Heuvelmans MA, Oudkerk M. Volume versus diameter assessment of small pulmonary nodules in CT lung cancer screening. *Transl Lung Cancer Res* 2017;6:52-61
38. Kim H, Park CM. Current perspectives for the size measurement of screening-detected lung nodules. *J Thorac Dis* 2018;10:1242-1244

 https://doi.org/10.3348/kjr.2020.0592